Earthquake Geotechnical Engineering for Protection and Development of Environment and Constructions – Silvestri & Moraci (Eds)
© 2019 Associazione Geotecnica Italiana, Rome, Italy, ISBN 978-0-367-14328-2

Field testing to evaluate the pore pressure response of liquefiable soil treated with earthquake drains

A. Marinucci
V2C Strategists LLC, Brooklyn, New York, USA

E.M. Rathje & K.H. Stokoe II
University of Texas at Austin, Austin, Texas, USA

ABSTRACT: Drainage methods represent one approach to mitigating liquefaction risk by reducing the distance of the drainage path (i.e., expediting drainage). In this paper, the design, execution, and results from a full-scale, dynamic field-testing program of a liquefiable site treated with prefabricated vertical drains (EQ-Drains) are presented and discussed. To evaluate the effectiveness of the EQ-Drains, accelerometers and pore pressure sensors were installed and monitored during dynamic loading. Before the full drain geometry was installed, significant excess pore pressures and shear strains were generated in the soil. During subsequent dynamic loading, excess pore pressure generation was considerably less. The vibratory installation of the EQ-Drains resulted in considerable and relatively immediate settlement within the area enveloped by the drains, which is a phenomenon not considered during design. Ultimately, it was determined that EQ-Drains were effective in accelerating the dissipation of excess pore water pressures when subjected to various levels of dynamic loading.

1 INTRODUCTION

Excess pore water pressures (Δu) are generated in saturated granular soil deposits when the soil is sheared, monotonically or dynamically, and these pressures are sustained when the rate of pore pressure generation is greater than the rate of dissipation. Liquefaction occurs when Δu equals the vertical effective stress (σ'_{v0}). Pore water pressures are eventually dissipated vertically, based on the hydraulic properties and drainage characteristics of the soil deposit. Assuming the ground surface is the only drainage boundary (i.e., no drainage elements present), Δu generated at some depth dissipates vertically upward. Upward pore water migration during dissipation may lead to a rise in groundwater elevation and liquefaction of shallower soils (i.e., due to a lower σ'_{v0}), even if these soils were initially unsaturated. Loss of strength becomes noticeable at values of pore pressure ratio ($r_u = \Delta u/\sigma'_{v0}$) as low as 0.5 to 0.6 (Seed et al 1975). In addition, this upward seepage may be impeded or prevented by the presence of interbedded layers of low permeability soils, which may lead to the development of a water film(s) or to "void redistribution-induced weakening of the soils at the interface" (Idriss & Boulanger 2008). The potential for liquefaction to occur can be somewhat reduced if the excess pore water pressure developed during shaking is even partially dissipated as it is being generated (Seed & Booker 1976, 1977).

Soil improvement methods have been used to minimize the consequences of liquefaction by changing the characteristics and/or response of a liquefiable soil deposit. Expediting drainage, which shortens the time of sustained Δu, represents one approach. By decreasing the drainage distance from vertically to radially between drains, vertical drains expedite the dissipation of Δu in an effort to maintain the value of Δu in the soil below a prescribed level. The true benefit of vertical drains may not be with preventing liquefaction from occurring but in reducing the overall time the soil remains in a liquefied state (Brennan & Madabhushi 2002). Therefore,

because Δu is reduced and/or dissipated relatively quickly, a corresponding reduction in the potential for strength loss, volume change, excessive settlement and deformation is realized.

Vertical drains can consist of either aggregate (i.e., gravel or crushed rock) or geo-composite elements, and are typically installed in a triangular or square grid pattern. The required spacing between vertical drains is a function of the design event, in-situ soil characteristics (most notably, hydraulic conductivity), and maximum allowable pore pressure ratio (r_u). For example, The Japanese Geotechnical Society (1998) recommends spacing the vertical drains such that the resulting predicted maximum average pore pressure ratio ($\overline{r_u}_{max}$) is no larger than 0.3. Depending on the construction method used to install the drains, some densification of the soil may occur (Idriss & Boulanger 2008). When the drains are installed using vibratory means, there likely will be densification of the in-situ soil around the drain; however, when the drains are installed by drilling and then filling, densification will be minimal or negligible. Regardless of type of vertical drain, flow through the soil is a function of the consolidation and drainage characteristics of the soil.

In this paper, full-scale dynamic field testing that was performed to evaluate the effectiveness of EQ-Drains to reduce excess pore pressures in liquefiable soil is described. To assess the effect on the soil properties, crosshole seismic testing was performed prior to and after the installation of the vertical drains. In addition, the ground surface was surveyed to determine the magnitude of the surface settlement caused by the vibratory installation of the vertical drains.

2 FIELD TESTING PROGRAM

2.1 *Prefabricated vertical drains*

Prefabricated vertical drains for earthquake mitigation (earthquake drains or EQ-Drains) comprise two elements: a slotted corrugated plastic pipe, with a typical nominal inside diameter of about 100 mm encased by a geotextile filter fabric, which minimizes the flow of soil into the EQ-Drain (Figure 1). Typically, for liquefaction remediation, EQ-Drains are installed in a triangular grid pattern with a center-to-center spacing ranging from 1.2 m to 2 m to a maximum depth of around 18 m. Moreover, EQ-Drains are typically installed using vibratory excitation, which densifies the in-situ soil deposit but does not provide any reinforcing effect. The key benefits of EQ-Drains over gravel drains include the inherent increased flow capacity and effective vertical hydraulic conductivity of the drain (due to its open inner diameter), which results in much greater flow area and less resistance to flow than for gravel drains. For the testing program in this study, 100-mm diameter EQ-Drains were installed in a triangular pattern with a spacing of 1.5 m.

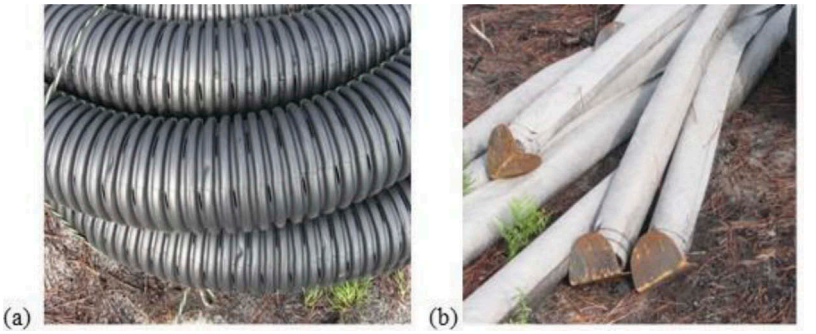

Figure 1. Photographs of a 100 mm diameter EQ-Drain: (a) bare and (b) with geotextile filter and base plate

2.2 *Subsurface conditions*

The field testing site was located in Conway, South Carolina, U.S.A. Cone penetration test (CPT) soundings and soil borings were advanced to a maximum depth of about 11 m. Three CPTs were performed in the area of the testing: CPTs A-12 and C-13 were performed prior to the EQ-Drain field testing in conjunction with the overall construction project and CPT T-1 was performed as a confirmatory sounding just prior to the testing. The distance between A-12 and C-13 was approximately 40 m, and CPT T-1 was positioned around the midpoint between A-12 and C-13. The generalized subsurface profile at the test site consisted of a layer of top soil with surface vegetation underlain by relatively clean, poorly graded (SP), loose-to-medium dense Pleistocene sand, which was underlain by a layer of silt and stiff clay at a depth of about 6 m. The subsurface profile at the testing location was highly variable and was inter-bedded with denser and looser layers. At the time of the testing, groundwater was found at a depth of about 0.6 m below the ground surface. The generalized subsurface profile and the CPT q_c (tip stress) profiles within the test area are provided in Figure 2.

2.3 *Experimental details*

Subsurface shaking and pore pressure generation was monitored via liquefaction sensors. A liquefaction sensor (Cox 2006) consists of: (1) a miniature pore water pressure transducer (mini-PPT) and (2) a tri-axial micro-electrical mechanical systems (MEMS) accelerometer and is approximately 38 mm in diameter by 127 mm in length. The mini-PPT was used to capture the change in pore water pressure during dynamic excitation and is approximately 25 mm in length and has a full-scale pressure range of 172 kPa. The MEMS accelerometer was used to capture the accelerations in the vertical (y) and horizontal (x, z) directions, are capacitance-based, and can capture both static and dynamic accelerations. The MEMS device is cube shaped with side dimensions of about 25 mm with a sensitivity range of ±2.5 V/g.

A vertically oriented, triangular array of sensors was installed in the test area to evaluate the ground response and pore water pressure generation and dissipation characteristics (Figure 3). The orientation used for the testing was such that the spatial axes (x, y, z) corresponded to the axes delineated on the MEMS accelerometer.

A tri-finned steel mandrel was used to install the EQ-Drains (Figure 4) and was also used as the dynamic excitation source because it was capable of inducing large cyclic shear strains in the soil deposit. The EQ-Drains were installed to a depth of about 6.1 m, which tipped the drains into the clay and silt layer underlying the sand. A vibratory hammer, with an operating

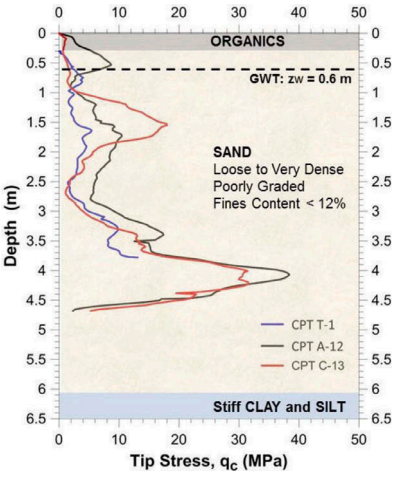

Figure 2. Generalized subsurface profile and CPT tip-stress profiles in the test area

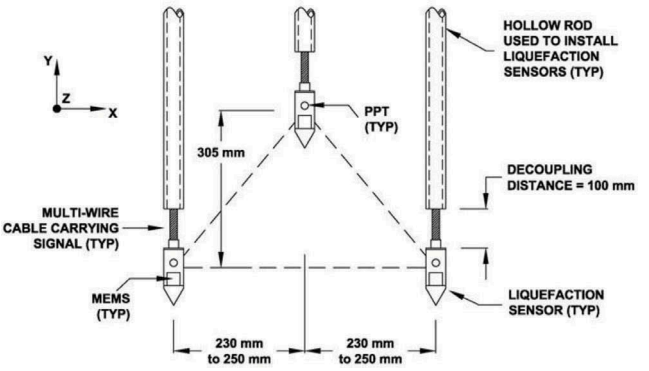

Figure 3. Spatial arrangement of the subsurface sensor array

frequency between 1400 and 1600 rpm (about 25 Hz), was mounted atop the steel mandrel and supplied the excitation for the testing program. The geometry of the mandrel and the transverse ribs on the mandrel itself added additional complexity to the shearing of the soil and to the emanating seismic wavefront, thereby inducing compression (P-wave), shear (S-wave), and Rayleigh waves during the advancing and withdrawal of the mandrel, which resulted in complex shearing of the soil.

The sensor array was placed at depths between 2.40 to 2.75 m below the ground surface (Figure 5), where q_c was equal to about 1.9 MPa representing a zone of minimum q_c within the upper portion of the sand layer and above the denser zone (Figure 2).

Crosshole seismic testing was performed to measure the in-situ shear wave velocity (V_s) of the soil and to assess, via compression wave velocity (V_p), whether the soil was saturated. The horizontal, in-plane component (x) and the vertical component (y) of the MEMS accelerometer in the sensors were used to capture the horizontally propagating compression wave velocity (V_P) and the horizontally propagating, vertically oriented shear wave velocity (V_S), respectively. The V_P of a saturated soil deposit is at least 1525 m/s. Based on the multiple

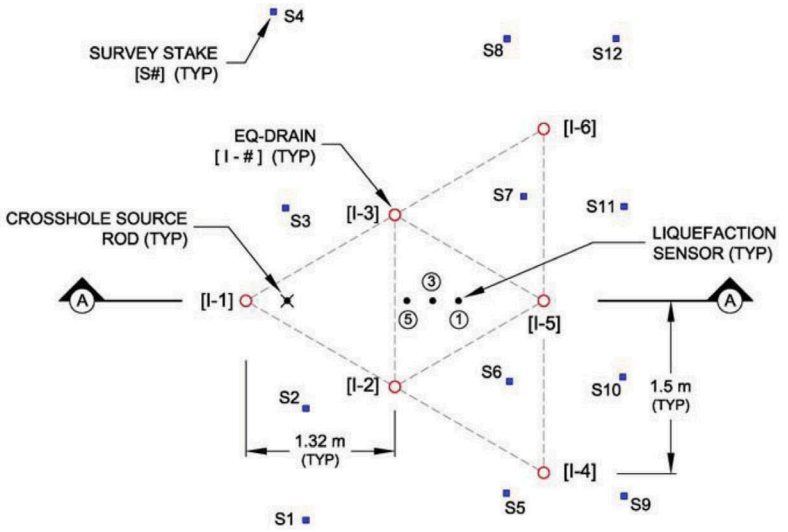

Figure 4. Plan view of the test area layout

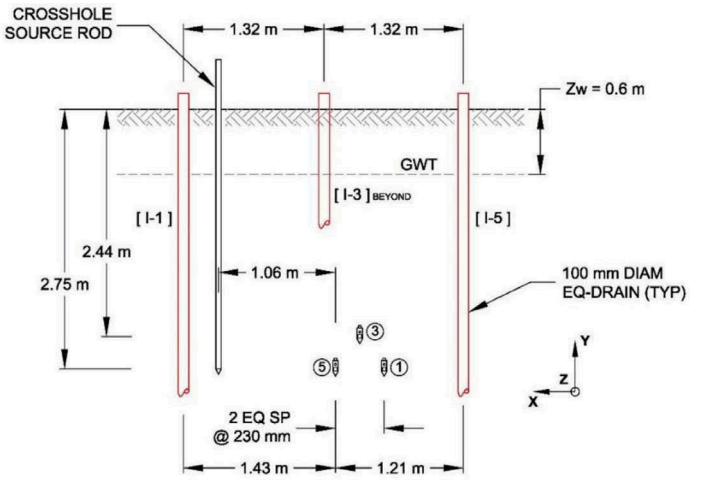

Figure 5. Cross-sectional view A-A through EQ-Drain I-1 to I-5 and centerline of the sensor array

Table 1. Initial shear wave velocity and CPT tip stress (based on CPT T-1)

Depth	Effective Stress	Shear Wave Velocity		CPT Tip Stress	
z (m)	σ'_{v0} (kPa)	Average V_S (m/s)	$V_{S,1}$ (m/s)	q_c (MPa)	$q_{C_{1N,cs}}$
2.7	32	152	202	1.9	74

crosshole seismic tests performed in the test area, it was determined that the soil was saturated below a depth of about 2 m.

The initial shear wave velocities and the CPT tip stresses in the sensor arrays in the test area are listed in Table 1, along with the stress-corrected shear wave velocity ($V_{S,1}$) and the normalized stress- and fines-corrected CPT tip resistance ($q_{c,1N_{CS}}$). Based on the average $V_{S,1}$, the soil was borderline liquefiable in ($V_{S,1}$~200 m/s) but based on the $q_{c,1N_{CS}}$ the soil was highly liquefiable. The discrepancy in determining the liquefaction susceptibility from shear wave velocity and CPT tip stress may be due to potential cementation of the Pleistocene sands at this site, which is a common phenomenon in the region. Shear wave velocity is more affected by cementation than CPT tip stress because shear waves induce very small strains, while advancing the CPT probe induces large strains that locally break the cementation.

3 EXPERIMENTAL RESULTS

Accelerations and pore pressure generation were monitored during installation of the EQ-Drains (I-1 to I-6 in Figure 4). In this way, the soil response during installation of EQ-Drains I-1 and I-2 represent the untreated response, and the installation of the subsequent EQ-Drains represent the response of the soil in the presence of adjacent drains and, potentially, some densification from the vibratory installation of the other drains.

For each sensor, the raw data set was recorded at a sampling frequency of 8192 samples/sec (Δt= 0.000122 s) and contained both pore water pressure and acceleration time histories. Each time history was zeroed so that each record would reflect only the excess pore pressure response from the dynamic excitation. The excess pore water pressure response was dominated by low frequencies; higher frequencies were also present in the signal and were filtered out

using a 54-Hz, low-pass, 10th order Butterworth filter. The acceleration response was dominated by high frequencies from the vibrations; lower frequency noise was filtered out using a 5-Hz, high-pass, 6th order Butterworth filter.

The excess pore pressure ratio (r_u) was computed by dividing the measured excess pore water pressure (Δu) by the estimated initial vertical effective stress (σ'_{v0}). Dynamic-displacement time histories were computed by double integrating the acceleration time histories and cyclic shear strains were computed from the relative displacements recorded between sensors using a 3-node triangular finite element interpolation scheme for shear strains in the *xy* vertical plane (γ_{xy}, Figure 5) and a 2-node strain displacement interpolation scheme for the *zy* vertical plane (γ_{yz}) and the *xz* horizontal plane (γ_{xz}). Computation of the shear strains in the three orthogonal planes was necessary due to the complex wave field generated by the vibrating mandrel and the different locations of the mandrel relative to the sensor array. Additional details can be found in Marinucci (2010).

For each of the installed drains, the average peak r_u across the three sensors and the peak cyclic shear strains are provided in Table 2. The r_u time histories generated during the installation of EQ-Drains I-1, I-2, I-3, and I-5 are shown in Figure 6 and the computed γ_{xy} are shown in Figure 7. The instances of rapid buildup in r_u for installation of I-1 (Figure 6a) are directly correlated to the instances of larger cyclic shear strains (Figure 7a). The maximum shear strain during the installation of I-1 was 0.026% in the *xy* vertical plane and generated very high r_u in PPT5 and PPT1 (locations shown in Figure 5), whereas significantly smaller r_u was recorded by PPT3 (Figure 6a). PPT3 was located at a shallower depth (about 305 mm higher) and may have been affected by partial saturation of the sensor or the soil. Nonetheless, as observed in Figure 6b, large values of r_u were recorded at PPT3 during installation of EQ-Drain I-2.

The peak cyclic shear strains in the *xy* vertical plane during the installation of I-1 were only slightly larger than the theoretical threshold cyclic shear strain value (i.e., γ_{max}~0.026% compared to γ_t^c~0.01%), but the values of r_u indicated liquefaction occurred. This result may have been affected by the large number of strain cycles induced (Figure 7), the combined effects of shearing on multiple planes, or by pore water pressure migration from other nearby looser sand. A similar pore pressure response was realized during the installation of EQ-Drain I-2 although the peak cyclic shear strains were noticeably greater (i.e., 2 to 3 times as large) due to the closer proximity of EQ-Drain I-2 to the sensor array (Figure 4). Although EQ-Drain I-1 had already been installed, the drain was far enough away to not influence the pore pressure response significantly.

It is interesting to compare the responses for the installation of EQ-Drains I-2 and I-3, which were located approximately equidistant from the sensor array but were located on opposite sides of the array. Larger cyclic shear strains were induced during installation of EQ-Drain I-3 but the r_u generated was significantly smaller and no residual pore pressure was present at the end of shaking. The smaller r_u for this case is due to the presence of, predominantly, EQ-Drain I-2, although it is also likely some densification occurred during installation of the earlier drains. During the installation of EQ-Drain I-3 (and all subsequent EQ-Drains), groundwater was observed flowing from the top of previously installed drains; therefore, significant pore pressures did not buildup in the ground. Only small-to-moderate excess pore

Table 2. Average peak r_u and peak shear strains generated during installation of the EQ-Drains

Installation of Drain	Duration of Shaking (sec)	Approx. Cycles of Shaking	Avg.$r_{u,max}$	Peak Shear Strain (%)		
				γ_{xy}	γ_{yz}	γ_{xz}
EQ-Drain I-1	52	1680	0.92	0.026	0.017	0.008
EQ-Drain I-2	72	2590	1.07	0.035	0.097	0.038
EQ-Drain I-3	77	2310	0.30	0.084	0.059	0.040
EQ-Drain I-4	84	2770	0.16	0.003	0.026	0.014
EQ-Drain I-5	61	2135	0.18	0.047	0.038	0.030
EQ-Drain I-6	72	2520	0.17	0.008	0.027	0.004

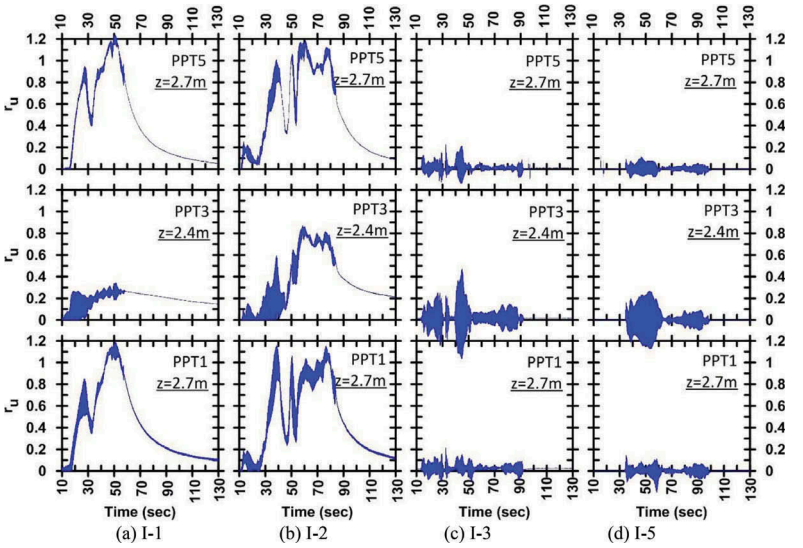

Figure 6. r_u time histories at the PPTs during installation of EQ-Drains

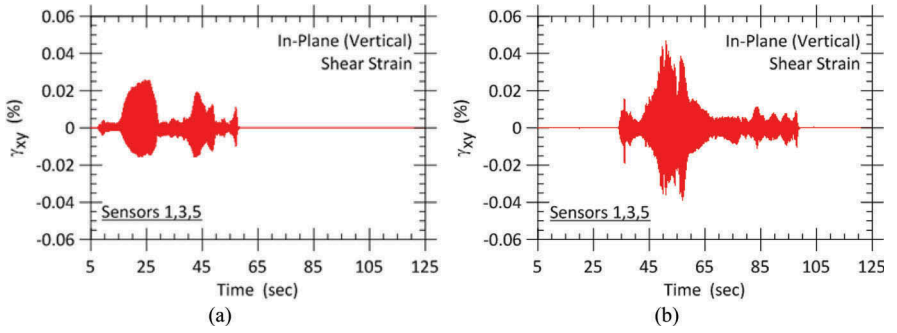

Figure 7. In-plane (γ_{xy}) cyclic shear strains during installation of EQ-Drain (a) I-1 and (b) I-5

water pressures were recorded within the array during the installation of EQ-Drains I-3 to I-6 (Table 2) and these pore pressure were only hydrodynamic (Figure 6) despite the induced cyclic shear strains being as large as other excitations (Table 2).

To assess the effect of the excitation events on the soil properties, crosshole seismic testing was performed soon after the installation of the last drain. The pre- and post-installation shear wave velocities measured from multiple crosshole seismic tests are presented in Table 3. Due to the installation of the drains, the shear wave velocity increased by about 45% at the depth of the sensor array.

The ground surface was optically surveyed using wooden stakes (S# on Figure 4) prior to installation of the EQ-Drains and at three additional times during the testing to evaluate the settlement caused by the various excitation events. The vertical strain (ε_v) at each stake location was computed by dividing the amount of vertical settlement (ΔH_v) by the maximum penetration depth of the steel mandrel (about 6.1 m). At the end of installation of the drains, the surveyed settlement ranged from 0.3 to 11 cm, with an average of about 7 cm, with the greatest amount of settlement being observed in the vicinity around EQ-Drain I-5. Correspondingly, the maximum vertical strain was about 1.9%, with an average of about 1.1%.

Table 3. Pre-installation and post-shaking average and stress-corrected shear wave velocities from crosshole seismic testing

Pre-Installation (*morning day 1*)			Post-Installation (*evening day 1*)	
Depth (m)	Avg. V_S (m/s)	V_{S1} (m/s)	Avg. V_S (m/s)	V_{S1} (m/s)
2.7	152	202	221	294

4 CONCLUSIONS

A full-scale in-situ experimental testing program was performed to evaluate the effectiveness of EQ-Drains in reducing the dynamic and excess pore water pressure response of a liquefiable site. In the test area, the vibratory installation of the first two EQ-Drains generated significant excess pore pressures; however, significant excess pore pressures (hydrodynamic or residual) were not generated during the vibratory installation of subsequent EQ-Drains due to the presence of the previously installed EQ-Drains. Moreover, the vibratory installation of the EQ-Drains caused significant settlement of the surface and altered the shear wave velocity of the sand. The results indicate that the EQ-Drains were effective at dissipating excess pore water pressures as well as densifying the site due to their installation.

REFERENCES

Brennan, A.J. and Madabhushi, S.P.G. (2002). "Effectiveness of vertical drains in mitigation of liquefaction," ASCE, *Soil Dynamics and Earthquake Eng'g*, Vol. 22, No. 9–12, p. 1059–1065.

Cox, B.R. (2006). *Development of a Direct Test Method for Dynamically Assessing the Liquefaction Resistance of Soils In Situ*, Ph.D. Dissertation, The University of Texas at Austin.

Idriss, I.M. and Boulanger, R.W. (2008). Soil Liquefaction during Earthquakes, Earthquake Engineering Research Institute (EERI) Monograph MNO-12, Oakland, CA.

Japanese Geotechnical Society (JGS), editor (1998). Remedial Measures against Soil Liquefaction: From Investigation to Implementation. A.A. Balkema, Rotterdam, The Netherlands.

Marinucci, A. (2010). *Effect of Prefabricated Vertical Drains on Pore Water Pressure Generation and Dissipation in Liquefiable Sand*, Ph.D. Dissertation, University of Texas at Austin.

Marinucci, A., Rathje, E.M., Ellington, J.S., Cox, B.R., Menq, F-Y, and Stokoe II, K.H. (2010). "Evaluation of the Effectiveness of Prefabricated Vertical Drains Using Full-Scale In Situ Staged Dynamic Testing." In *Art of Foundation Engineering Practice - Proceedings of the Art of Foundation Engineering Practice Congress 2010*. ASCE Geotechnical Special Publication No. 198. p. 380–394.

Seed, H.B. and Booker, J.R. (1976). "Stabilization of Potentially Liquefiable Sand Deposits Using Gravel Drain Systems," Report No. EERC 76–10, Earthquake Engineering Research Center, University of California, Berkeley.

Seed, H.B. and Booker, J.R. (1977). "Stabilization of Potentially Liquefiable Sand Deposits Using Gravel Drains," ASCE, Journal of the Geotechnical Engineering Division, Vol. 103, No. GT7, p. 757–768.

Seed, H.B., Martin, P.P. and Lysmer, J. (1975). "The Generation and Dissipation of Pore Water Pressures during Soil Liquefaction," Report No. EERC 75–26, Earthquake Engineering Research Center, University of California, Berkeley.

Silicon Designs, Inc. (2004). "Technical Specifications for Triaxial Analog Accelerometer Module, Model 2430."

S&ME, Inc.. (2006). Design Geotechnical Exploration Report. S&ME Project No. 1633-06-680.

Youd, T.L., Idriss, I.M., Andrus, R.D., Arango, I., Castro, G., Christian, J.T., Dobry, R., Finn, W.D.L., Harder, L.F., Jr., Hynes, M.E., Ishihara, K., Koester, J.P., Liao, S.S.C., Marcuson, W.F., III, Martin, G.R., Mitchell, J.K., Moriwaki, Y., Power, M.S., Robertson, P.K., Seed, R.B., and Stokoe, K.H., II. (2001). "Liquefaction Resistance of Soils: Summary Report from the 1996 NCEER and 1998 NCEER/NSF Workshops on Evaluation of Liquefaction Resistance of Soils," ASCE, *Journal of Geotechnical and Geoenvironmental Engineering*, Vol. 127, No. 10, p. 817–833.